Molecular Pharmacology Fast Forward. Published on May 18, 2007 as DOI: 10.1124/mol.107.036418
This article has not been copyedited and formatted. The final version may differ from this version.

MOL #36418

Inhibition of Hypoxia-Induced Increase of Blood-Brain Barrier Permeability by YC-1 through the Antagonism of HIF-1α Accumulation and VEGF Expression

WEI-LAN YEH, DAH-YUU LU, CHUN-JUNG LIN, HOUNG-CHI LIOU and

WEN-MEI FU

Department of pharmacology (W.-L.Y., D.-Y.L., H.-C.L., W.-M.F.) and Graduate Institute of Pharmaceutical Science (C.-J.L.), College of Medicine, National Taiwan University, Taipei, Taiwan

Molecular Pharmacology Fast Forward. Published on May 18, 2007 as DOI: 10.1124/mol.107.036418
This article has not been copyedited and formatted. The final version may differ from this version.

Running title: Inhibition of BBB permeability by YC-1

Corresponding author: Wen-Mei Fu, Department of pharmacology, College of Medicine, National Taiwan University, No. 1, Sec. 1, Jen-Ai Road, Taipei, Taiwan.

E-mail: wenmei@ntu.edu.tw

The number of text pages: 37; The number of figures: 9; The number of references: 40

The number of words in the *Abstract*: 193; The number of words in the *Introduction*: 638; The number of words in the *Discussion*: 946

ABBREVIATIONS:

CNS, central nervous system; $CoCl_2$, cobalt chloride; BBB, blood-brain barrier; DMSO, dimethyl sulfoxide; EBD, Evans blue dye; FITC-dextran, Fluorescein isothiocyanate-dextran; HIF-1α, hypoxia inducible factor-1alpha; HRE, hypoxia-response elements; KT5823, 9-methoxy-9-methoxycarbonyl-8-methyl-2,3,9,10-tetrahydro-8,11-epxoy-1H,8H,11H-2,7b-11a-triazadibenzo(a,g)cycloocta(cde)-trinden-1-one; L-NAME, L-nitro-arginine-methyl easterase; MCAO, middle cerebral artery occlusion; MTT, 3--2,5- diphenyltetrazolium bromide; ODQ, 1H-[1,2,4]oxadiazolo[4,3-a]quinoxalin-1-one; PBS, phosphate-buffered saline; PKG, protein kinase G; sGC, soluble quanylate cyclase; TJ, tight junction; VEGF, vascular endothelial growth factor; YC-1, 3-(5'-hydroxymethyl-2'-furyl)-1-benzylindazole; ZO-1, zonular occludens-1; cGMP, (3,5) cyclic quanosine monophosphate

Molecular Pharmacology Fast Forward. Published on May 18, 2007 as DOI: 10.1124/mol.107.036418
This article has not been copyedited and formatted. The final version may differ from this version.

Abstract

Cerebral microvascular endothelial cells form the anatomical basis of the blood-brain barrier (BBB), and the tight junctions of the BBB are critical for maintaining brain homeostasis and low permeability. Ischemia/reperfusion is known to damage the tight junctions of BBB and lead to permeability changes. Here we investigated the protective role of YC-1, 3-(5'-hydroxymethyl-2'-furyl)-1-benzylindazole, against chemical hypoxia and hypoxia/reoxygenation (H/R)-induced BBB hyperpermeability using adult rat brain endothelial cell culture (ARBEC). YC-1 significantly decreased $CoCl_2$- and H/R-induced hyperpermeability of FITC-dextran in cell culture inserts. It was found that the decrease and disorganization of tight junction protein ZO-1 in response to $CoCl_2$ and H/R was antagonized by YC-1. The protection of YC-1 may result from the inhibition of HIF-1α accumulation and production of its downstream target VEGF. VEGF alone significantly increased FITC-dextran permeability and down-regulated mRNA and protein levels of ZO-1 in ARBECs. We further used animal model to examine the effect of YC-1 on BBB permeability after cerebral ischemia/reperfusion. It was found that YC-1 significantly protected the BBB against ischemia/reperfusion-induced injury. Taken together, these results indicate that YC-1 may inhibit HIF-1α accumulation and VEGF production, which in turn protect BBB from injury caused by hypoxia.

Introduction

Pathological conditions such as tumors, inflammation, and ischemia are known to damage the BBB and lead to the increase of permeability and development of vasogenic brain edema, and VEGF is likely to be a candidate to regulate the change of permeability (Schoch et al., 2002). Using *in vitro* model of the blood-brain barrier (BBB) consisting of brain microvascular endothelial cells, hypoxia-induced hyperpermeability is mediated by the VEGF/VEGF receptor system in an autocrine manner (Fischer et al., 1999). Increase of vascular permeability and subsequent inflammatory responses may contribute to pathogenetic cofactors responsible for the development of neurological damage.

The blood-brain barrier constructed from brain microvessel endothelial cells forms a metabolic and physical barrier to protect the central nervous system (CNS) from the compositional fluctuations that occur in the blood. Blood-brain barrier, which is different from peripheral microvascular endothelium, is due to the presence of tight junctions (TJs) between neighboring endothelial cells. Tight junctions are complexes of transmembrane proteins that connect to the cytoarchitecture via membrane-associated accessory proteins. Claudin family and occludin are integral transmembrane proteins. Both of these proteins have multiple transmembrane domains and interact with adjacent cells to form homodimeric bridges (Feldman et al.,

Molecular Pharmacology Fast Forward. Published on May 18, 2007 as DOI: 10.1124/mol.107.036418
This article has not been copyedited and formatted. The final version may differ from this version.

2005). Stabilization of TJs involves a network of claudins and occludin linked to the actin cytoskeleton via the zonular occludens proteins (ZO-1, ZO-2 and ZO-3). ZO proteins are membrane-associated accessory proteins which mediate the linkage between actin and the cytoplasmic tail of claudins and occludin (Gloor et al., 2001). Moreover, ZO proteins are members of membrane-associated guanylate kinase (MAGUK) family conserved guanylate kinase domain, an SH3 domain and multiple PDZ domains, suggesting that ZO proteins may participate in signal transduction cascade (Gonzalez-Mariscal et al., 2000).

HIF-1 is a heterodimer composed of two subunits—HIF-1α (120kDa) and HIF-1β (91-94kDa)—which are basic helix-loop-helix (bHLH) protein of the PAS (Per-ARNT-AHR-Sim) family (Wang et al., 1995). HIF-1α is ubiquitinated by von Hippel-Lindau (VHL) protein and subjected to proteasomal degradation in non-hypoxic cells, whereas HIF-1β is expressed constitutively in all cells (Salceda and Caro, 1997). Exposure of cells to hypoxia or transition metals like cobalt and iron chelators induces HIF-1α expression and inhibits HIF-1α ubiquitination by dissociating VHL from HIF-1α. HIF-1α comprises a bHLH domain near the amino (N) terminal, which is essential for DNA binding to hypoxia-response elements (HREs) in the HIF target genes such as vascular endothelial growth factor (VEGF), endothelin-1 (ET-1), and erythropoietin (EPO) (Sharp and Bernaudin, 2004).

Molecular Pharmacology Fast Forward. Published on May 18, 2007 as DOI: 10.1124/mol.107.036418
This article has not been copyedited and formatted. The final version may differ from this version.

VEGF, also named vascular permeability factor (VPF), is one of the most well-known HIF target gene involved in vascular biology (Forsythe et al., 1996). Effects of VEGF on the endothelial cells are evidently mediated by high affinity cell surface receptors, VEGFR-1 and VEGFR-2. Thus, endothelial cells have a unique and specific spectrum of responses to VEGF (Connolly, 1991). Although many recent reports focused on the angiogenic effect of VEGF, VEGF was initially discovered as a tumor-secreted factor that increases vascular permeability (Senger et al., 1983). During vascular sprouting, cell junctions are partially disorganized, which allows endothelial cells to migrate and proliferate and also increase vascular permeability (Dejana, 2004; Dvorak et al., 1995).

YC-1, 3-(5'-hydroxymethyl-2'-furyl)-1-benzylindazole, was first introduced to increase NO-soluble guanylate cyclase (sGC) activity and cGMP level on platelets (Ko et al., 1994). However, YC-1-mediated responses via cGMP-independent pathway have also been reported (Chien et al., 2005; Hsu et al., 2003). In addition, a growing evidence suggests that YC-1 exerts a novel inhibitory effect on the accumulation of HIF-1α, which in turn blocks the expression of VEGF and anti-angiogenesis (Yeo et al., 2003; Yeo et al., 2004). Here, we examined whether YC-1 inhibits the destruction and hyperpermeability of BBB induced by cobalt, hypoxia/reoxygenation or ischemia/reperfusion. We demonstrated that YC-1

Molecular Pharmacology Fast Forward. Published on May 18, 2007 as DOI: 10.1124/mol.107.036418
This article has not been copyedited and formatted. The final version may differ from this version.

significantly inhibits HIF-1α accumulation and VEGF production caused by hypoxia treatment in ARBECs. The *in vivo* study also reveals that YC-1 is able to protect BBB from ischemia/reperfusion-induced injury.

Molecular Pharmacology Fast Forward. Published on May 18, 2007 as DOI: 10.1124/mol.107.036418
This article has not been copyedited and formatted. The final version may differ from this version.

Materials and methods

Materials

YC-1 was provided by Yung-Shin Pharmaceutical Industry Co. Ltd. (Taichung, Taiwan). DMSO, served as vehicle was purchased from Sigma (St. Louis, MO). $CoCl_2$, a hypoxia mimetic agent, was purchased from Wako (Japan). Recombinant human VEGF, goat anti-rat VEGF antibody, and goat control IgG antibody were purchased from R&D systems (Minneapolis, MN).

Cell cultures

Immortalized ARBECs (adult rat brain endothelial cells) is a generous gift from National Research Council Canada (Garberg et al., 2005). ARBECs were seeded onto 75 cm^2 flasks coated with type I rat tail collagen (50 μg/ml, Sigma, St. Louis, MO) and maintained in M199 (Gibco, Grand Island, NY, USA) containing 1% D-glucose solution, 1% BME amino acid solutions, 1% BME vitamin solutions (Sigma, St. Louis, MO), 100 U/mL penicillin and 100 mg/mL streptomycin, 10% heat-inactivated fetal bovine serum (FBS; Hyclone, Logan, UT, USA) at 37°C in a humidified incubator under 5% CO_2 and 95% air. Confluent cultures were passaged by trypsinization. Cells from passage 35~45 were used and starved overnight before experiments.

Hypoxia-reoxygenation of cultured ARBECs

Molecular Pharmacology Fast Forward. Published on May 18, 2007 as DOI: 10.1124/mol.107.036418
This article has not been copyedited and formatted. The final version may differ from this version.

To induce hypoxia, confluent monolayers of ARBEC cultures were placed into special chamber (Anaerobic System PROOX model 110; BioSpherix), which was closed and placed inside an incubator at 37°C and gassing the special chamber with a gas mixture consisting of 95% N_2, 5% CO_2. After 24 hr, cell cultures were moved out of the hypoxia chamber and reoxygenated in a regular normoxic incubator (95% air, 5% CO_2) for another 4 hr. For comparison, control cultures were incubated under normoxic conditions for the same duration.

Cell viability assay

Cell viability was assessed by MTT assay. ARBECs cultured onto 24-well plate coated with type I rat tail collagen were induced chemical hypoxia using $CoCl_2$, or suffered an H/R insult in the presence or absence of YC-1. Culture medium was aspirated 24 hr after treatment and MTT (0.5 mg/ml; Sigma, St. Louis, MO) was added in each well. MTT was then removed 30 min later and cells were lysed by DMSO. The absorbance was measured at 550 nm by microplate reader (Bio-Tek, Winooski, VT).

Assay of paracellular permeability

The permeability assay using cell culture insert system was performed as described previously (Andriopoulou et al., 1999) with minor modifications. ARBECs $4x10^4$ were seeded onto cell culture inserts (diameter: 10 mm, pore size: 0.4 μm

Molecular Pharmacology Fast Forward. Published on May 18, 2007 as DOI: 10.1124/mol.107.036418
This article has not been copyedited and formatted. The final version may differ from this version.

polycarbonate membrane; Nalge Nunc international, NY, USA) coated with type I rat tail collagen (50 μg/ml, 100μl). When cultured cells were confluent, FITC-dextran (1mg/ml, 500μl, average molecular mass, 43,200; Sigma, St. Louis, MO) was then added into the upper compartment followed by adding $CoCl_2$ or putting into hypoxia chamber in the absence or presence of YC-1. At the indicated time points, 50 μl sample medium was taken from the lower compartment. After a dilution of the sample medium to 500 μl with PBS, fluorescence intensity of FITC-dextran was measured at 492 nm excitation and 520 nm emission wavelengths by a fluorescent reader (Spectra MAX Gemini XS).

Western blot analysis

ARBECs were seeded onto 6 cm dishes coated with type I rat tail collagen. Cells were exposed to drugs for 6 or 24 hr for detection of HIF-1α or TJ proteins, respectively. After washing with cold PBS, cells were lysed with radioimmunoprecipitation assay buffer (RIPA; 200 μl/dish) on ice for 30 min. After centrifugation at 18,000g for 20 min, the supernatant was used for Western blotting. Protein concentration was measured by BCA assay kit (Pierce, Rockford, IL) with BSA as a standard. Equal proteins (30 μg for TJ proteins and 80 μg for HIF-1α) were separated on 8% sodium dodecyl sulphate-polyacrylamide gels and transferred to polyvinylidene difluoride (PVDF) membranes (Millipore, Bedford, MA, USA). The membranes were incubated

for 1 h with 4% dry skim milk in PBS buffer to block nonspecific binding and then incubated with rabbit antibodies against occludin (1:1000; Santa Cruz Biotechnology, CA), claudin-1, ZO-1 (1:1000; Zymed, CA), or mouse antibodies against HIF-1α (1:1000; Novus Biologicals, Littleton, CO, USA), α-tubulin (1:1000; Santa Cruz Biotechnology, CA) for 1 hr. After PBST washing, the membranes were then incubated with goat anti-rabbit or anti-mouse peroxidase-conjugated secondary antibody (1:1000; Santa Cruz Biotechnology) for 1 h. The blots were visualized by enhanced chemiluminescence (ECL; Santa Cruz Biotechnology, CA) using Kodak X-OMAT LS film (Eastman Kodak, Rochester, NY).

Immunocytofluorescent staining

ARBECs were seeded onto glass overslips coated with type I rat tail collagen. After exposure to drugs for 24 hr, cells were washed with PBS and fixed with PBS containing 4% paraformaldehyde for 15 min, and then permeabilized with 1% Triton X-100 for 20min. After blocking with 4% dry skim milk in PBS buffer, cells were incubated with rabbit antibodies against ZO-1 (1:100) overnight at 4°C. Following a brief wash, cells were then incubated with goat anti-rabbit FITC-conjugated secondary antibody (1:200; Leinco Tec. Inc., St. Louis, MO) for 1 h. Finally, cells were washed again, mounted, and visualized with Zeiss fluorescence microscope.

Molecular Pharmacology Fast Forward. Published on May 18, 2007 as DOI: 10.1124/mol.107.036418
This article has not been copyedited and formatted. The final version may differ from this version.

Transfection and reporter gene assay

ARBECs were seeded onto 12-well plate coated with type I rat tail collagen. Cells were co-transfected with 0.4 μg lac-Z vector, and 0.8 μg HRE-luciferase reporter gene, 1.5 kb VEGF-luciferase reporter gene or 1.2 kb HRE-deleted VEGF-luciferase reporter gene, respectively (gifts from M.L. Kuo, National Taiwan University, Taipei, Taiwan). Plasmid DNA and Lipofectamine 2000 (LF2000; 10 μg/ml; Invitrogen) were premixed with Opti-MEM I (Gibco, Grand Island, NY) separately for 5 min and then mix with each other for 25 min and then applied to the cells (500 μl/well). After 24 hr's transfection, the medium was replaced with fresh serum-free culture medium and exposed to drugs for 24 hr for the detection of HRE-luciferase and VEGF-luciferase activity. To prepare lysates, 100 μl reporter lysis buffer (Promega, Madison, WI) was added to each well, and cells were scraped from plates. The supernatant was collected after centrifugation at 15,000g for 3 min. Aliquots of cell lysates (20 μl) containing equal amounts of proteins were placed into wells of an opaque white 96-well microplate. The luciferase activity was determined using a dual-luciferase reporter assay system (Promega) and activity value was normalized to transfection efficiency monitored by the co-transfected lacZ vector.

Reverse transcriptase-PCR and quantitative real time-PCR

Molecular Pharmacology Fast Forward. Published on May 18, 2007 as DOI: 10.1124/mol.107.036418
This article has not been copyedited and formatted. The final version may differ from this version.

ARBECs were seeded onto 6-well plate coated with type I rat tail collagen. After exposure to drugs for 6 or 24 hr, total RNA were extracted using a TRIzol kit (MDBio, Inc., Taipei, Taiwan). 2 μg RNA were used for reverse transcription by using a commercial kit (Invitrogen; Carlsbad, CA). PCR was performed using an initial step of denaturation (5 min at 95°C), 30 cycles of amplification (95°C for 30 sec, 60°C for 1 min, and 72°C for 30 sec), and an extension (72°C for 2 min). PCR products were analyzed on 2% agarose gels. Quantitative real time-PCR was proceeded using SYBR Green I Master Mix and analyzed with a model 7900 Sequence Detector System (Applied Biosystems; Foster City, CA). After pre-incubation at 50°C for 2 min and 95°C for 10 min, the PCR was performed as 40 cycles of 95°C for 10 sec and 60°C for 1 min. The threshold was set above the nontemplate control background and within the linear phase of target gene amplification to calculate the cycle number at which the transcript was detected (denoted as C_T). The oligonucleotide primers were:

ZO-1: forward: 5’-GCGAGGCATCGTTCCTAATAAG-3’ and

reverse: 5’-TCGCCACCTGCTGTCTTTG-3’;

VEGF: forward: 5'-ACGAAAGCGCAAGAAATCCC-3’ and

reverse: 5’-TTAACTCAAGCTGCCTCGCC-3’;

β-actin: forward: 5’-AGGCTCTTTTCCAGCCTTCCT-3’ and

reverse: 5’-GTCTTTACGGATGTCAACGTCACA-3’.

Molecular Pharmacology Fast Forward. Published on May 18, 2007 as DOI: 10.1124/mol.107.036418
This article has not been copyedited and formatted. The final version may differ from this version.

Enzyme-linked immunosorbent assay

ARBECs were seeded onto 24-well plate coated with type I rat tail collagen. After exposure to drugs for 24 hr, 100 μl of culture medium was collected and frozen at -80°C until measurement by Quantikine Rat VEGF Immunoassay ELISA kit (R&D systems, Minneapolis, MN). After adding 50 μl Assay Diluent into each microplate well, 50 μl of sample medium was then added and incubated for 2 hr at room temperature on the shaker. Following a brief wash, 100 μl Conjugate buffer were added and incubated for 1 hr. Finally, 100 μl Substrate Solution were added and incubated in dark, and 100 μl Stop Solution were added 30 min after. The absorbance was measured at 450 nm by an ELISA reader (Bio-Tek, Winooski, VT).

Increase of blood-brain barrier permeability by ischemia-reperfusion in rat

Male Sprague-Dawley rats were obtained from the National Laboratory Animal Center of Taiwan and kept on a 12-h light/dark cycle with *ad libitum* access to food and water. Rats were acclimated to their environment for 7 days before the experiments. The rats (250~300 g) were then anesthetized with trichloroacetaldehyde (400 mg/kg) and two common carotid arteries were exposed and occluded by artery clips through a neck skin incision. Under an operating microscope, a piece of skull was removed through a head skin incision, and middle cerebral artery (MCA) was tied with a polyamide monofilament non-absorbable suture (diameter: 150 microns;

Johnson & Johnson) to produce ischemia, and rectal temperature was maintained at 37°C by external warming. 1.5 hr after occlusion, YC-1 (1 mg/kg) was injected from femoral vein just before untying of suture. Evans blue dye (100 mg/kg; Sigma, St. Louis, MO) was injected from femoral vein 2 hr after reperfusion. Rats were perfused with saline 4 hr later through the left ventricle until colorless perfusion fluid was obtained from the right atrium. After decapitation, the brain was removed from the skull and each hemicortex were dissected.

Samples were weighed and soaked in 1 ml of 50% Trichloroacetic acid solution. After homogenization and centrifugation, the extracted Evans blue dye was diluted with ethanol (1:3), and fluorescence intensity was measured at 620 nm excitation and 680 nm emission wavelengths using a fluorescence reader (Belayev et al., 1996). The tissue content of Evans blue dye was quantified from a linear standard curve derived from known amounts of the dye and was expressed as μg/g tissue.

Immunohistochemistry

After ischemia/reperfusion, rats were anesthetized and perfused with saline and fixed with phosphate buffer containing 4% paraformaldehyde. After decapitation, the brain was removed from the skull, postfixed in 4% paraformaldehyde at 4°C overnight, and then stored in 30% sucrose solution at 4°C for 2 days. Frozen samples were cut into slices by a sliding microtome in 50-μm-thick coronal sections. Brain slices were

Molecular Pharmacology Fast Forward. Published on May 18, 2007 as DOI: 10.1124/mol.107.036418
This article has not been copyedited and formatted. The final version may differ from this version.

rinsed with PBS, and then soaked in 3% H_2O_2 (Wako, Tokyo, Japan) solution for 15 min to block endogenous peroxidase activity. After blocking in 10% dry skim milk containing 0.5% Triton X-100 for 1 hr, slices were incubated with mouse antibodies against HIF-1α (1:100; Chemicon, Temecula, CA) overnight at 4°C. Following a brief wash, slices were then incubated with horse anti-mouse biotinylated secondary antibodies, and processed with avidin–biotin complex system (Vector; Burlingame, CA), which was visualized by incubating with 0.5 mg/ml diaminobenzidine-HCl (DAB; Sigma, St. Louis, MO) and 0.01% H_2O_2 in PBS. The DAB reaction was stopped by rinsing slices with PBS.

Statistics

Values are expressed as mean ± SEM of at least three experiments. Results were analyzed with one-way analysis of variance (ANOVA), followed by Neuman-Keuls. Significance was defined as $p < 0.05$.

Molecular Pharmacology Fast Forward. Published on May 18, 2007 as DOI: 10.1124/mol.107.036418
This article has not been copyedited and formatted. The final version may differ from this version.

Results

Inhibition by YC-1 on increase of paracellular permeability and destruction of ZO-1 in response to either $CoCl_2$ or hypoxia/reoxygenation treatment in ARBECs.

Exposure of ARBECs to chemical hypoxia-inducing agent $CoCl_2$ (100μM) resulted in a significant increase (1.82-fold) of paracellular permeability within 24 hr compared with control, and this effect was quantified by measuring FITC-dextran flux through paracellular monolayers in culture insert system after 24 hr's treatment (Fig. 1). It was found that pretreatment with YC-1 (10μM) for 30 min inhibited $CoCl_2$-induced increase of paracellular permeability, whereas YC-1 alone did not affect the paracellular flux of FITC-dextran. Total amounts of FITC-dextran collected in the lower compartment of culture insert system after 24 hr revealed that YC-1 inhibited $CoCl_2$-induced increase of permeability by 80.0±4.8% (n=4). In addition, 24hr's hypoxia followed by 4 hr's reoxygenation (H/R) also significantly increased paracellular permeability, and YC-1 (10 μM) pretreatment antagonized H/R-induced increase of paracellular permeability by 68.4±8.0% (n=4). To confirm the increase of permeability is not due to cytotoxicity, cell viability was assessed by MTT. There was no significant difference in viability after drug treatment.

To determine whether $CoCl_2$- and H/R-induced increase of paracellular

Molecular Pharmacology Fast Forward. Published on May 18, 2007 as DOI: 10.1124/mol.107.036418
This article has not been copyedited and formatted. The final version may differ from this version.

permeability was due to alteration in the expression of TJ proteins, ZO-1, occludin, and claudin-1 expression levels were examined by Western blotting. As shown in Fig. 2A, treatment with $CoCl_2$ reduced ZO-1 protein expression levels by 51.4±11.8% (n=4), and pretreatment of YC-1 antagonized $CoCl_2$-induced reduction of ZO-1 expression in a concentration-dependent manner. Furthermore, as shown in Fig.2D, ZO-1 protein expression levels following H/R were reduced by 53.1±5.8%, and pretreatment of 10μM YC-1 also antagonized H/R-induced reduction of ZO-1 expression. However, $CoCl_2$, H/R, or YC-1 treatment exerted no significant effect on occludin and claudin-1 (Fig. 2, B, C, E, & F).

To examine the structural basis for the alteration in permeability, the distribution of ZO-1 was visualized by immunofluorescent staining. The result also revealed that the arrangement of ZO-1 was disorganized in response to $CoCl_2$ or H/R treatment and YC-1 antagonized the destruction of ZO-1 (Fig. 3). These results were consistent with the inhibitory effect of YC-1 on FITC-dextran permeability as shown in Fig. 1, indicating that YC-1 is capable of inhibiting $CoCl_2$- and H/R-induced ZO-1 destruction and increase of paracellular permeability.

Inhibition by YC-1 on $CoCl_2$-induced increase of paracellular permeability in ARBECs is not through cGMP and PKG pathway.

Since YC-1 has been characterized as nitric oxide (NO) sensitizer, and regulates

Molecular Pharmacology Fast Forward. Published on May 18, 2007 as DOI: 10.1124/mol.107.036418
This article has not been copyedited and formatted. The final version may differ from this version.

intracellular cGMP concentration through the enhancement of sensitivity of soluble guanylate cyclase to NO (Chien et al., 2005), we then examined whether the inhibitory effect of YC-1 was through NO-cGMP-PKG pathway. It was found that L-NAME (non-selective NOS inhibitor; 0.5mM) attenuated the protective effect of YC-1 in response to $CoCl_2$ treatment. However, co-treatment with 20μM ODQ (sGC inhibitor) or 1μM KT5823 (PKG inhibitor) did not antagonize the protective effect of YC-1 against $CoCl_2$-induced hyperpermeability (Fig. 4A). In addition, treatment of 30μM 8-Br-cGMP also did not exert the similar effect as YC-1 to inhibit ZO-1 destruction following $CoCl_2$ treatment (Fig. 4B). These results suggest that cGMP and PKG is not involved in the protective action of YC-1.

Inhibition by YC-1 on $CoCl_2$-induced HIF-1α accumulation and VEGF production in ARBECs.

It is well known that $CoCl_2$ exposure results in the upregulation of HIF-1α and downstream target gene expression in many cell types (Gleadle et al., 1995; Ke et al., 2005). We then investigated the effect of YC-1 on HIF-1α accumulation in ARBECs. ARBECs were pretreated with different concentrations of YC-1 for 30 min and then exposed to $CoCl_2$ (100 μM) for another 6 hr. As shown in Fig. 5A, Western blotting demonstrated that $CoCl_2$-induced HIF-1α accumulation was inhibited by YC-1 in a concentration-dependent manner. In addition, we also examined $CoCl_2$-induced

Molecular Pharmacology Fast Forward. Published on May 18, 2007 as DOI: 10.1124/mol.107.036418
This article has not been copyedited and formatted. The final version may differ from this version.

enhancement of HIF-1 activity by using HRE-luciferase reporter gene. ARBECs were transfected with reporter gene and were then exposed to $CoCl_2$ in the absence or presence of YC-1 for another 24 hr. Cell lysates were prepared, and the luciferase activities were analyzed. As shown in Fig. 5B, $CoCl_2$-induced increase of HRE-luciferase activity was also concentration-dependently inhibited by YC-1.

Since VEGF is one of the well-known downstream target gene of HIF-1 related to vascular biology (Forsythe et al., 1996; Sharp and Bernaudin, 2004), we then investigated whether VEGF is involved in the protective effect of YC-1 against $CoCl_2$-induced increase of paracellular permeability in ARBECs. First of all, we demonstrated that $CoCl_2$ treatment increased VEGF-luciferase activity when cells were transfected with full length of VEGF-luciferase reporter gene (1.5 kb) but not with HRE-deleted VEGF-luciferase reporter gene (1.2 kb; Fig. 6A). This result confirmed the stimulating effect of $CoCl_2$ on VEGF expression is through HIF-1 binding to HRE promoter region of VEGF gene (Ema et al., 1997; Liu et al., 1995). Furthermore, it was found that 1.5 kbVEGF-luciferase activity enhanced by $CoCl_2$ treatment was antagonized by YC-1 in a concentration-dependent manner (Fig. 6B). Pretreatment of YC-1 (10 μM) also inhibited $CoCl_2$-induced VEGF mRNA expression by using quantitative real time-PCR measurement (Fig. 6C). Furthermore, VEGF protein content in cultured medium measured by ELISA kit revealed that there

Molecular Pharmacology Fast Forward. Published on May 18, 2007 as DOI: 10.1124/mol.107.036418
This article has not been copyedited and formatted. The final version may differ from this version.

was a significant increase (4.0-fold) after 24 hr exposure of $CoCl_2$ compared with control (160.7±25.4 pg/10^5 cells and 40.1±0.7 pg/10^5 cells, respectively), which was abolished by YC-1 treatment (46.1±6.2 pg/10^5 cells; Fig. 6D). These results indicate that HIF-1α accumulation and VEGF production in response to chemical hypoxia is inhibited by YC-1 in ARBECs.

Involvement of VEGF in the increase of paracellular permeability and destruction of ZO-1 following either $CoCl_2$ or H/R treatment in ARBECs.

It has been reported that BBB permeability is increased by VEGF (Schoch et al., 2002), we then examined whether VEGF production affects ZO-1 expression. We evaluated the expression levels of protein as well as mRNA. It was found that VEGF (20 ng/ml), $CoCl_2$ or H/R treatment reduced ZO-1 protein expression, however, VEGF antibody administration antagonized the ZO-1 reduction caused by $CoCl_2$ exposure or H/R treatment (Fig. 7A, 7B), while IgG administration was served as negative control. In addition, treatment of VEGF for 6 hr or treatment with $CoCl_2$ for 24 hr reduced ZO-1 mRNA expression by 45.2±12.0% and 44.9±8.3%, respectively. The reduction in ZO-1 mRNA expression in response to $CoCl_2$ was abolished by concomitant treatment with YC-1 (Fig. 7C). We further examined the effect of VEGF antibody on the permeability potentiating action of $CoCl_2$ or H/R treatment. As shown in Fig. 7D, VEGF (20 ng/ml) used to serve as positive control was found to increase

Molecular Pharmacology Fast Forward. Published on May 18, 2007 as DOI: 10.1124/mol.107.036418
This article has not been copyedited and formatted. The final version may differ from this version.

FITC-dextran flux through paracellular monolayers by 2.1-fold. Exposure of ARBECs to either $CoCl_2$ or H/R increased the paracellular permeability by 1.8-fold and 1.7-fold, respectively, and VEGF antibody inhibited $CoCl_2$- or H/R-induced an increase of paracellular permeability by 46.0±6.9% and 53.2±7.5% (n=4), respectively. This result indicates that $CoCl_2$ or H/R caused an increase of paracellular permeability, which may result from the enhancement of VEGF production.

To further examine the structural basis for the alteration in permeability, the distribution of ZO-1 was visualized by immunofluorescent staining. The result reveals that VEGF antibody antagonized the destruction of ZO-1 in response to $CoCl_2$ or H/R treatment (Fig. 8), which is consistent with the effect of antibody on permeability increase. These results indicate that VEGF is involved in $CoCl_2$ or H/R-induced an increase of paracellular permeability and destruction of ZO-1 in ARBECs.

Inhibition by YC-1 on ischemia/reperfusion-induced increase of BBB permeability and HIF-1α accumulation in rats.

The results mentioned above show that YC-1 exerts protection of ARBECs against $CoCl_2$- or H/R-induced an increase of paracellular permeability *in vitro*, we then investigated whether YC-1 exerts protective effect *in vivo*. Rats were ligated in bilateral common carotid arteries and one MCA for 1.5 hr and reperfused for 6 hr. Evans blue dye was used to serve as a marker of albumin extravasation. As shown in

Fig. 9A, ipsilateral side but not contralateral side exhibited a marked increase (9.5-fold) of permeability (20.35±3.62 μg/g tissue and 2.15±0.97 μg/g tissue, respectively) (Belayev et al., 1996). Treatment of YC-1 strongly reduced the increase of permeability by 76.8% (5.35 ± 1.52 μg/g tissue; Fig. 9B). Furthermore, immunostaining demonstrated that ischemia/reperfusion increased HIF-1α accumulation in both cerebral blood vessels (arrowhead) and non-vascular cells (Fig. 9C, middle panel), and administration of YC-1 inhibited the accumulation of HIF-1α (Fig. 9C, lower panel). These results indicate that YC-1 is able to protect BBB from hyperpermeability induced by ischemia/reperfusion in animal model.

Molecular Pharmacology Fast Forward. Published on May 18, 2007 as DOI: 10.1124/mol.107.036418
This article has not been copyedited and formatted. The final version may differ from this version.

Discussion

Tight junction barrier in endothelial cells of cerebral microvasculature serves as a frontline defense, protecting neurons and glia cells from harmful insults. Under pathological conditions, tight junction proteins may undergo rearrangement or alteration in protein expression (Mark and Davis, 2002; Wang et al., 2001). Hypoxia is an important pathogenic factor for the alteration of tight junction proteins and induction of vascular leakage in the brain. It has been reported that the dominant negative form of HIF-1α inhibits the hypoxia-induced activity of VEGF promoter in Hep3B cells (Forsythe et al., 1996), and exposure to hypoxia leads to a significant increase of VEGF mRNA and protein in mouse brain, which is correlated with the severity of the hypoxia (Schoch et al., 2002). It is also found that hypoxia-induced hyperpermeability of brain microvascular endothelial cell monolayers is mediated by VEGF in an autocrine manner (Fischer et al., 1999). Here we found that hypoxia caused an increase of BBB endothelial permeability and a destruction of ZO-1 partially by acting through HIF-1α-induced VEGF production. However, other tight junction proteins, such as occludin and claudin-1, are not affected. We also found that VEGF inhibits ZO-1 mRNA expression, indicating that VEGF regulates ZO-1 expression at the transcription level. This result is consistent with that reported by Ghassemifar *et al* (2006), i.e. VEGF has a dual capability with respect to the

regulation of the expression of some TJ proteins at the transcriptional and post-translational levels on different cell types. However, the exact mechanisms regarding the regulation on VEGF production and VEGF-mediated expression of TJ proteins by HIF-1α still require further investigation. Here we demonstrate that YC-1 is able to abolish these harmful effects in response to hypoxia through inhibition of HIF-1α accumulation and VEGF production. Other factors except VEGF may also contribute to hypoxia-induced hyperpermeability because YC-1 is much more effective than VEGF antibody in the inhibition of permeability.

In addition to the protective action of YC-1 in cell cultures, *in vivo* study also reveals that YC-1 is able to inhibit ischemia/reperfusion-induced an increase of BBB permeability in rats. Nevertheless, the responses in animal study may be more complicated and focus on a single intracellular pathway or cell type might not be sufficient. The neurovascular unit composes of endothelial cells, astrocytes, pericytes, adjacent neurons, extracellular matrix and basal lamina (Hawkins and Davis, 2005). After ischemia/reperfusion, perturbations in neurovascular functional integrity initiate several cascades of injury. Upstream signals such as oxidative stress, together with neutrophil and/or platelet interactions with activated endothelium, upregulate matrix metalloproteinases (MMPs), plasminogen activators, other proteases and inflammatory cytokines, which degrade matrix and lead to the increase of BBB

permeability (Hawkins and Davis, 2005; Lo et al., 2003). Thus, the origin of protective effects of YC-1 other than endothelial cells in animal studies can not be excluded. Using VEGF inhibitor or neutralizing antibody may also be useful to certify the protective effect in ischemia/reperfusion rats.

YC-1 is not only a suppressor of HIF-1α accumulation (Kim et al., 2006), but also a NO sensitizer. YC-1 regulates intracellular cGMP concentration through the enhancement of sensitivity of soluble guanylate cyclase to NO (Ko et al., 1994). On one hand, NO has emerged as an important regulator in controlling vascular tone (Shesely et al., 1996). However, there are controversies regarding its role in the modulation of microvascular permeability. There are some evidences to support that activation of nitric oxide synthase (NOS) and NO production results in an increase of microvascular permeability in response to hypoxia (Mark et al., 2004) or inflammatory mediators (Bove et al., 2001), whereas other reports demonstrate that NO is a permeability-decreasing factor and maintain junctional integrity (Kurose et al., 1994; Predescu et al., 2005). Furthermore, there are also disputes about the role of cGMP/PKG in vascular permeability. Some evidences support that cGMP has a barrier-enhancing effect (Moldobaeva et al., 2006) and protect microvessel from ROS-induced injury (Pearse et al., 2003), while others considered cGMP as a permeability-increasing factor no matter under the normoxic or hypoxic conditions

(Fischer et al., 1999). Our results show that L-NAME (NOS inhibitor) attenuated the protective effect of YC-1 in response to $CoCl_2$-induced injury. However, co-treatment with ODQ or KT5823 (sGC inhibitor and PKG inhibitor, respectively) did not affect the protective effect of YC-1, and treatment of 8-Br-cGMP did not exert similar protection as YC-1. These results indicate that NO but not cGMP or PKG is an additional protective effector to reduce $CoCl_2$-induced BBB permeability.

In addition to VEGF, other factors may also contribute to barrier dysfunction, such as TGF-β. TGF-β can be up-regulated under hypoxia through HIF-1α and increases endothelial permeability through the reorganization of adherence junctions and focal adhesion complexes (Lu et al., 2006). Furthermore, many evidences indicate that there is crosstalk between growth factors, and cell signaling might escape from one pathway to aggravate another compensatory pathway. Expression of VEGF and VEGF receptor were increased by TGF-β, and MMP expression, which can be activated by hypoxia (Jeon et al., 2007). Since HIF-1α is a transcription factor acting upstream of many factors regulating hypoxic response in many cell types, we therefore consider that HIF-1α inhibitor may have more therapeutic benefit in preventing BBB destruction and brain edema in patients suffering from stroke, as compared to either VEGF inhibitor alone or agents targeting tight junctions.

In summary, the results from this study clearly demonstrate that ARBECs

Molecular Pharmacology Fast Forward. Published on May 18, 2007 as DOI: 10.1124/mol.107.036418
This article has not been copyedited and formatted. The final version may differ from this version.

undergo molecular and functional changes under hypoxia, and these phenomena can be abolished by the treatment of YC-1. Furthermore, YC-1 protects BBB from ischemia/reperfusion-induced hyperpermeability in animal model, and inhibits HIF-1α accumulation in cerebral blood vessels and non-vascular cells. Therefore, YC-1 may have the potential to be developed as a novel drug to inhibit the increase of BBB permeability following ischemia.

Molecular Pharmacology Fast Forward. Published on May 18, 2007 as DOI: 10.1124/mol.107.036418
This article has not been copyedited and formatted. The final version may differ from this version.

Acknowledgements

We thank National Research Council Canada for providing us the cell line ARBECs.

References

Andriopoulou P, Navarro P, Zanetti A, Lampugnani MG and Dejana E (1999) Histamine induces tyrosine phosphorylation of endothelial cell-to-cell adherens junctions. *Arteriosclerosis, thrombosis, and vascular biology* **19**(10):2286-2297.

Belayev L, Busto R, Zhao W and Ginsberg MD (1996) Quantitative evaluation of blood-brain barrier permeability following middle cerebral artery occlusion in rats. *Brain Res* **739**(1-2):88-96.

Bove K, Neumann P, Gertzberg N and Johnson A (2001) Role of ecNOS-derived NO in mediating TNF-induced endothelial barrier dysfunction. *Am J Physiol Lung Cell Mol Physiol* **280**(5):L914-922.

Chien WL, Liang KC, Teng CM, Kuo SC, Lee FY and Fu WM (2005) Enhancement of learning behaviour by a potent nitric oxide-guanylate cyclase activator YC-1. *The European journal of neuroscience* **21**(6):1679-1688.

Connolly DT (1991) Vascular permeability factor: a unique regulator of blood vessel function. *Journal of cellular biochemistry* **47**(3):219-223.

Dejana E (2004) Endothelial cell-cell junctions: happy together. *Nature reviews* **5**(4):261-270.

Dvorak HF, Brown LF, Detmar M and Dvorak AM (1995) Vascular permeability

factor/vascular endothelial growth factor, microvascular hyperpermeability, and angiogenesis. *The American journal of pathology* **146**(5):1029-1039.

Ema M, Taya S, Yokotani N, Sogawa K, Matsuda Y and Fujii-Kuriyama Y (1997) A novel bHLH-PAS factor with close sequence similarity to hypoxia-inducible factor 1alpha regulates the VEGF expression and is potentially involved in lung and vascular development. *Proceedings of the National Academy of Sciences of the United States of America* **94**(9):4273-4278.

Feldman GJ, Mullin JM and Ryan MP (2005) Occludin: structure, function and regulation. *Advanced drug delivery reviews* **57**(6):883-917.

Fischer S, Clauss M, Wiesnet M, Renz D, Schaper W and Karliczek GF (1999) Hypoxia induces permeability in brain microvessel endothelial cells via VEGF and NO. *The American journal of physiology* **276**(4 Pt 1):C812-820.

Forsythe JA, Jiang BH, Iyer NV, Agani F, Leung SW, Koos RD and Semenza GL (1996) Activation of vascular endothelial growth factor gene transcription by hypoxia-inducible factor 1. *Molecular and cellular biology* **16**(9):4604-4613.

Garberg P, Ball M, Borg N, Cecchelli R, Fenart L, Hurst RD, Lindmark T, Mabondzo A, Nilsson JE, Raub TJ, Stanimirovic D, Terasaki T, Oberg JO and Osterberg T (2005) In vitro models for the blood-brain barrier. *Toxicol In Vitro* **19**(3):299-334.

Ghassemifar R, Lai CM and Rakoczy PE (2006) VEGF differentially regulates transcription and translation of ZO-1alpha+ and ZO-1alpha- and mediates trans-epithelial resistance in cultured endothelial and epithelial cells. *Cell and tissue research* **323**(1):117-125.

Gleadle JM, Ebert BL, Firth JD and Ratcliffe PJ (1995) Regulation of angiogenic growth factor expression by hypoxia, transition metals, and chelating agents. *The American journal of physiology* **268**(6 Pt 1):C1362-1368.

Gloor SM, Wachtel M, Bolliger MF, Ishihara H, Landmann R and Frei K (2001) Molecular and cellular permeability control at the blood-brain barrier. *Brain research* **36**(2-3):258-264.

Gonzalez-Mariscal L, Betanzos A and Avila-Flores A (2000) MAGUK proteins: structure and role in the tight junction. *Seminars in cell & developmental biology* **11**(4):315-324.

Hawkins BT and Davis TP (2005) The blood-brain barrier/neurovascular unit in health and disease. *Pharmacological reviews* **57**(2):173-185.

Hsu HK, Juan SH, Ho PY, Liang YC, Lin CH, Teng CM and Lee WS (2003) YC-1 inhibits proliferation of human vascular endothelial cells through a cyclic GMP-independent pathway. *Biochemical pharmacology* **66**(2):263-271.

Jeon SH, Chae BC, Kim HA, Seo GY, Seo DW, Chun GT, Kim NS, Yie SW, Byeon

WH, Eom SH, Ha KS, Kim YM and Kim PH (2007) Mechanisms underlying TGF-beta1-induced expression of VEGF and Flk-1 in mouse macrophages and their implications for angiogenesis. *Journal of leukocyte biology* **81**(2):557-566.

Ke Q, Kluz T and Costa M (2005) Down-regulation of the expression of the FIH-1 and ARD-1 genes at the transcriptional level by nickel and cobalt in the human lung adenocarcinoma A549 cell line. *International journal of environmental research and public health [electronic resource]* **2**(1):10-13.

Kim HL, Yeo EJ, Chun YS and Park JW (2006) A domain responsible for HIF-1alpha degradation by YC-1, a novel anticancer agent. *International journal of oncology* **29**(1):255-260.

Ko FN, Wu CC, Kuo SC, Lee FY and Teng CM (1994) YC-1, a novel activator of platelet guanylate cyclase. *Blood* **84**(12):4226-4233.

Kurose I, Wolf R, Grisham MB and Granger DN (1994) Modulation of ischemia/reperfusion-induced microvascular dysfunction by nitric oxide. *Circulation research* **74**(3):376-382.

Liu Y, Cox SR, Morita T and Kourembanas S (1995) Hypoxia regulates vascular endothelial growth factor gene expression in endothelial cells. Identification of a 5' enhancer. *Circulation research* **77**(3):638-643.

Lo EH, Dalkara T and Moskowitz MA (2003) Mechanisms, challenges and opportunities in stroke. *Nat Rev Neurosci* **4**(5):399-415.

Lu Q, Harrington EO, Jackson H, Morin N, Shannon C and Rounds S (2006) Transforming growth factor-beta1-induced endothelial barrier dysfunction involves Smad2-dependent p38 activation and subsequent RhoA activation. *J Appl Physiol* **101**(2):375-384.

Mark KS, Burroughs AR, Brown RC, Huber JD and Davis TP (2004) Nitric oxide mediates hypoxia-induced changes in paracellular permeability of cerebral microvasculature. *American journal of physiology* **286**(1):H174-180.

Mark KS and Davis TP (2002) Cerebral microvascular changes in permeability and tight junctions induced by hypoxia-reoxygenation. *American journal of physiology* **282**(4):H1485-1494.

Moldobaeva A, Welsh-Servinsky LE, Shimoda LA, Stephens RS, Verin AD, Tuder RM and Pearse DB (2006) Role of protein kinase G in barrier-protective effects of cGMP in human pulmonary artery endothelial cells. *Am J Physiol Lung Cell Mol Physiol* **290**(5):L919-930.

Pearse DB, Shimoda LA, Verin AD, Bogatcheva N, Moon C, Ronnett GV, Welsh LE and Becker PM (2003) Effect of cGMP on lung microvascular endothelial barrier dysfunction following hydrogen peroxide. *Endothelium* **10**(6):309-317.

Predescu D, Predescu S, Shimizu J, Miyawaki-Shimizu K and Malik AB (2005) Constitutive eNOS-derived nitric oxide is a determinant of endothelial junctional integrity. *Am J Physiol Lung Cell Mol Physiol* **289**(3):L371-381.

Salceda S and Caro J (1997) Hypoxia-inducible factor 1alpha (HIF-1alpha) protein is rapidly degraded by the ubiquitin-proteasome system under normoxic conditions. Its stabilization by hypoxia depends on redox-induced changes. *The Journal of biological chemistry* **272**(36):22642-22647.

Schoch HJ, Fischer S and Marti HH (2002) Hypoxia-induced vascular endothelial growth factor expression causes vascular leakage in the brain. *Brain* **125**(Pt 11):2549-2557.

Senger DR, Galli SJ, Dvorak AM, Perruzzi CA, Harvey VS and Dvorak HF (1983) Tumor cells secrete a vascular permeability factor that promotes accumulation of ascites fluid. *Science* **219**(4587):983-985.

Sharp FR and Bernaudin M (2004) HIF1 and oxygen sensing in the brain. *Nat Rev Neurosci* **5**(6):437-448.

Shesely EG, Maeda N, Kim HS, Desai KM, Krege JH, Laubach VE, Sherman PA, Sessa WC and Smithies O (1996) Elevated blood pressures in mice lacking endothelial nitric oxide synthase. *Proceedings of the National Academy of Sciences of the United States of America* **93**(23):13176-13181.

Wang GL, Jiang BH, Rue EA and Semenza GL (1995) Hypoxia-inducible factor 1 is a basic-helix-loop-helix-PAS heterodimer regulated by cellular O2 tension. *Proceedings of the National Academy of Sciences of the United States of America* **92**(12):5510-5514.

Wang W, Dentler WL and Borchardt RT (2001) VEGF increases BMEC monolayer permeability by affecting occludin expression and tight junction assembly. *American journal of physiology* **280**(1):H434-440.

Yeo EJ, Chun YS, Cho YS, Kim J, Lee JC, Kim MS and Park JW (2003) YC-1: a potential anticancer drug targeting hypoxia-inducible factor 1. *Journal of the National Cancer Institute* **95**(7):516-525.

Yeo EJ, Chun YS and Park JW (2004) New anticancer strategies targeting HIF-1. *Biochemical pharmacology* **68**(6):1061-1069.

Footnotes

The work was supported by research grants from the National Science Council of Taiwan.

Molecular Pharmacology Fast Forward. Published on May 18, 2007 as DOI: 10.1124/mol.107.036418
This article has not been copyedited and formatted. The final version may differ from this version.

Legends for figures

Figure 1. Inhibition by YC-1 on $CoCl_2$- or H/R-induced an increase of paracellular permeability in ARBECs.

ARBECs cultured in cell culture inserts were pretreated with YC-1 (10 μM) for 30 min and then either treated with $CoCl_2$ (100 μM) for another 24 hr or exposed to 24 hr's hypoxia followed by 4 hr's reoxygenation (H/R). Leakage of FITC-dextran were collected in the lower compartment. The data represent the mean ± SEM from four independent experiments. *, $p<0.05$, as compared with control group. #, $p<0.05$, as compared with $CoCl_2$-treated group or H/R group.

Figure 2. Antagonism by YC-1 on the reduction of ZO-1 proteins in response to $CoCl_2$ or H/R treatments.

ARBECs pretreated with different concentrations of YC-1 were then either exposed to $CoCl_2$ (100 μM) for another 24 hr (A, B, C) or suffered from 24 hr's hypoxia following by 4 hr's reoxygenation (D, E, F). Cell lysates were prepared and followed by electrophoresis and immunoblotting for the determination of protein levels of ZO-1 (A, D), occludin (B, E), and claudin-1 (C, F). The data represent the mean ±

SEM from at least three independent experiments. *, $p<0.05$, compared with control group. #, $p<0.05$, compared with $CoCl_2$- or H/R-treated group.

Figure 3. Effect of YC-1 on the destruction of ZO-1 in response to $CoCl_2$ or H/R treatments.

ARBECs grown on coverslips were pretreated with YC-1 (10 μM) for 30 min and then either exposed to $CoCl_2$ (100 μM) for another 24 hr or 24 hr's hypoxia following by 4 hr's reoxygenation. Immunofluorescence of ZO-1 in control (A), YC-1 alone (B), $CoCl_2$ treatment (C), $CoCl_2$ plus YC-1 (D), H/R treatment (E), and H/R puls YC-1 (F). Scale bar, 5μm.

Figure 4. Inhibition by YC-1 on $CoCl_2$-induced an increase of paracellular permeability in ARBECs is not through cGMP and PKG.

(A) ARBECs were cultured in cell culture inserts and pretreated with YC-1 (10 μM) for 30 min and then exposed to $CoCl_2$ (100 μM). Leakage of FITC-dextran were collected in the lower compartment after 24 hr's treatment of $CoCl_2$. (B) ARBECs were pretreated with 8-Br-cGMP (30 μM) for 30 min and then exposed to $CoCl_2$ (100 μM)

Molecular Pharmacology Fast Forward. Published on May 18, 2007 as DOI: 10.1124/mol.107.036418
This article has not been copyedited and formatted. The final version may differ from this version.

for another 24 hr. Cell lysates were prepared and followed by electrophoresis and immunoblotting for the determination of protein levels of ZO-1. Note that L-NAME but not ODQ or KT5823 attenuates the protective effect of YC-1 in response to $CoCl_2$-induced injury. Treatment of 8-Br-cGMP did not exert the similar protective effect as YC-1. The data represent the mean ± SEM from at least three independent experiments. *, $p<0.05$, compared with control group. #, $p<0.05$, compared with $CoCl_2$-treated group. ϕ, $p<0.05$, compared with $CoCl_2$ + YC-1 group.

Figure 5. Inhibition by YC-1 on $CoCl_2$-induced HIF-1α accumulation in endothelial cells.

(A) ARBECs were pretreated with different concentrations of YC-1 for 30 min and then exposed to $CoCl_2$ (100 μM) for another 24 hr. Cell lysates were prepared and followed by electrophoresis and immunoblotting for the determination of protein levels of HIF-1α. (B) Cells co-transfected with HRE-luciferase reporter gene and lac-Z vector were exposed to $CoCl_2$ with or without different concentrations of YC-1. The data represent the mean ± SEM from at least three independent

Molecular Pharmacology Fast Forward. Published on May 18, 2007 as DOI: 10.1124/mol.107.036418
This article has not been copyedited and formatted. The final version may differ from this version.

experiments. *, $p<0.05$, compared with control group. #, $p<0.05$, compared with $CoCl_2$-treated group.

Figure 6. Inhibition by YC-1 on $CoCl_2$-induced VEGF production in endothelial cells.

(A) Increase of VEGF-luciferase activity by $CoCl_2$ (100 μM) was observed by transfection with full length of VEGF-luciferase reporter gene (1.5 kb) but not with HRE-deleted VEGF-luciferase reporter gene (1.2 kb). (B) Cells co-transfected with 1.5 kb or 1.2 kb VEGF-luciferase reporter gene and lac-Z vector were exposed to $CoCl_2$ in the presence or absence of YC-1. Note that YC-1 antagonized the increase of VEGF reporter gene activity and VEGF mRNA expression induced by $CoCl_2$ (C). (D) Culture medium was collected for the measurement of VEGF using ELISA kit after treatment with YC-1 (10 μM) plus $CoCl_2$ (100 μM) for 24 hr. The data represent the mean ± SEM from at least three independent experiments. *, $p<0.05$, compared with control group. #, $p<0.05$, compared with $CoCl_2$-treated group.

Figure 7. Involvement of VEGF in $CoCl_2$- or H/R-induced an increase of

Molecular Pharmacology Fast Forward. Published on May 18, 2007 as DOI: 10.1124/mol.107.036418
This article has not been copyedited and formatted. The final version may differ from this version.

paracellular permeability.

ARBECs were either (A) exposed to $CoCl_2$ (100 μM) or (B) suffered from H/R in the presence or absence of VEGF antibody (Ab, 1 μg/ml) for indicated time intervals. IgG antibody (IgG, 1 μg/ml) or VEGF (20 ng/ml) treatment was used as negative and positive control, respectively. Cell lysates were prepared after treatment and protein levels of ZO-1 were determined. (C) Cell lysates were prepared after 6 or 24 hr treatment of $CoCl_2$ and followed by reverse transcriptase-PCR for the determination of mRNA levels of ZO-1. Note that $CoCl_2$-induced an increase of VEGF is involved in permeability increase, which is antagonized by concomitant treatment with YC-1. (D) In cell culture insert systems, leakage of FITC-dextran were collected in the lower compartment after 24 hr's $CoCl_2$ treatment or 24 hr's hypoxia following by 4 hr's reoxygenation. The data represent the mean ± SEM from at least three independent experiments. *, $p<0.05$, compared with control group. #, $p<0.05$, compared with $CoCl_2$- or H/R-treated group.

Figure 8. Involvement of VEGF in the destruction of ZO-1 arrangement in response to $CoCl_2$ or H/R treatment.

Molecular Pharmacology Fast Forward. Published on May 18, 2007 as DOI: 10.1124/mol.107.036418
This article has not been copyedited and formatted. The final version may differ from this version.

ARBECs grown on coverslips were either treated with $CoCl_2$ (100 μM) for 24 hr or exposed to 24 hr's hypoxia following by 4 hr's reoxygenation in the absence (C, D) or presence (G, H) of VEGF antibody (1 μg/ml). IgG antibody (1 μg/ml) was used as negative control (E, F). Note that compared with control (A), both $CoCl_2$ or H/R treatment caused the destruction of ZO-1 (C, D), which was inhibited by co-administration of VEGF antibody (G, H). VEGF (20 ng/ml) treatment alone was used as positive control (B). Scale bar, 5μm.

Figure 9. Inhibition by YC-1 on ischemia/reperfusion-induced an increase of BBB permeability and HIF-1α accumulation in rats.

(A) Right middle cerebral artery and two common carotid arteries were transiently ligated for 1.5 hr and YC-1 (1 mg/kg) was injected from femoral vein just before reperfusion. Evans blue dye (100 mg/kg) was injected from femoral vein 2 hr after reperfusion, and permeability was evaluated 4 hr later. Scale bar, 1cm. (B) Evans blue dye was extracted from each hemicortex as a marker of albumin extravasation. (C) Immunostaining of HIF-1α shows that ischemia/reperfusion (I/R) increased the immunostaining of HIF-1α in cerebral blood vessels

Molecular Pharmacology Fast Forward. Published on May 18, 2007 as DOI: 10.1124/mol.107.036418
This article has not been copyedited and formatted. The final version may differ from this version.

(arrowhead) and non-vascular cells (middle panel). Administration of YC-1 inhibited the accumulation of HIF-1α (lower panel). Scale bar, 50μm. The data represent the mean ± SEM ($n \geqq 9$). *, $p<0.05$, compared with I/R group.

Figure 1.

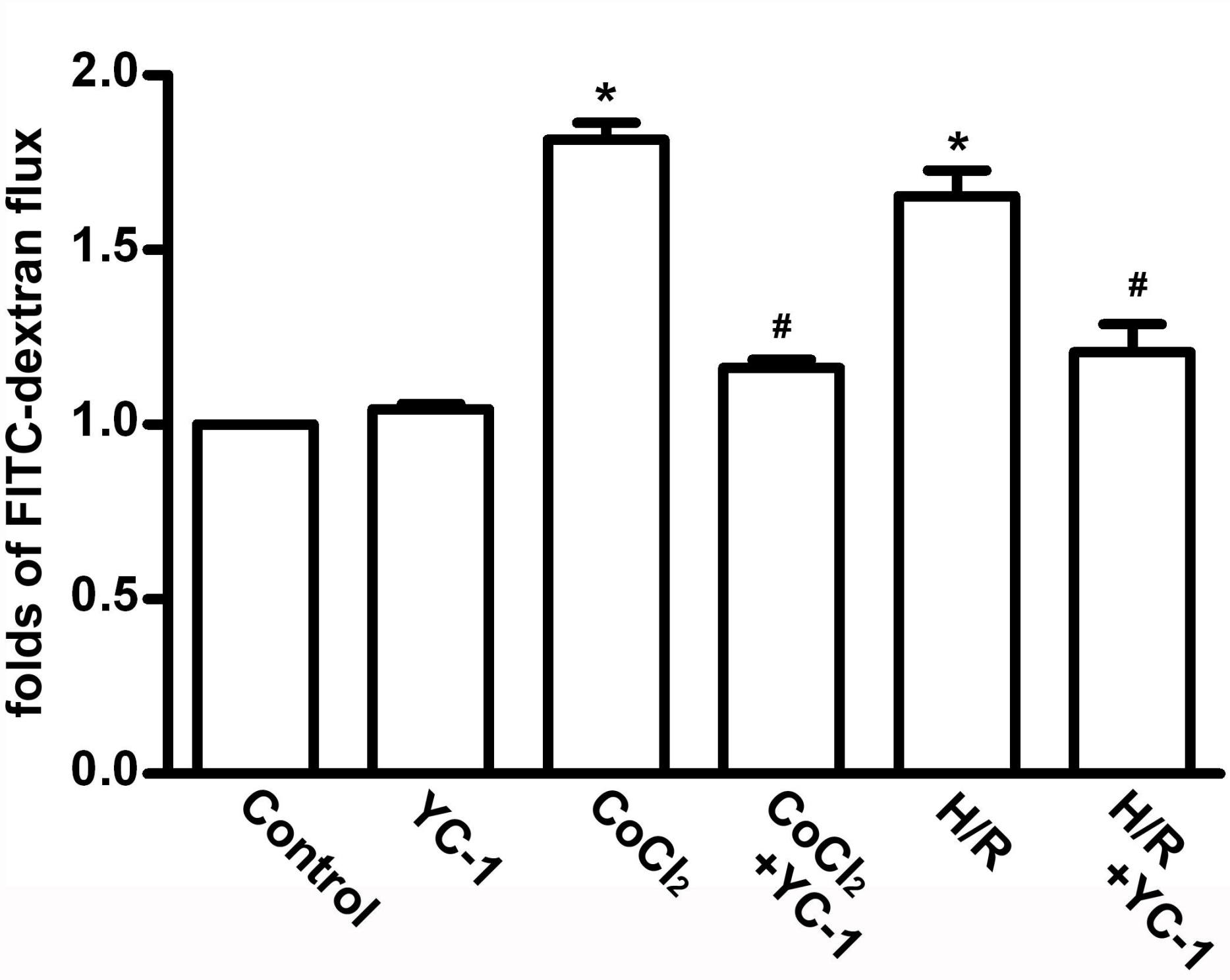
folds of FITC-dextran flux
2.0
1.5
1.0
0.5
0.0
*
*
#
#
Control
YC-1
CoCl2
CoCl2 +YC-1
H/R
H/R +YC-1

Figure 2.

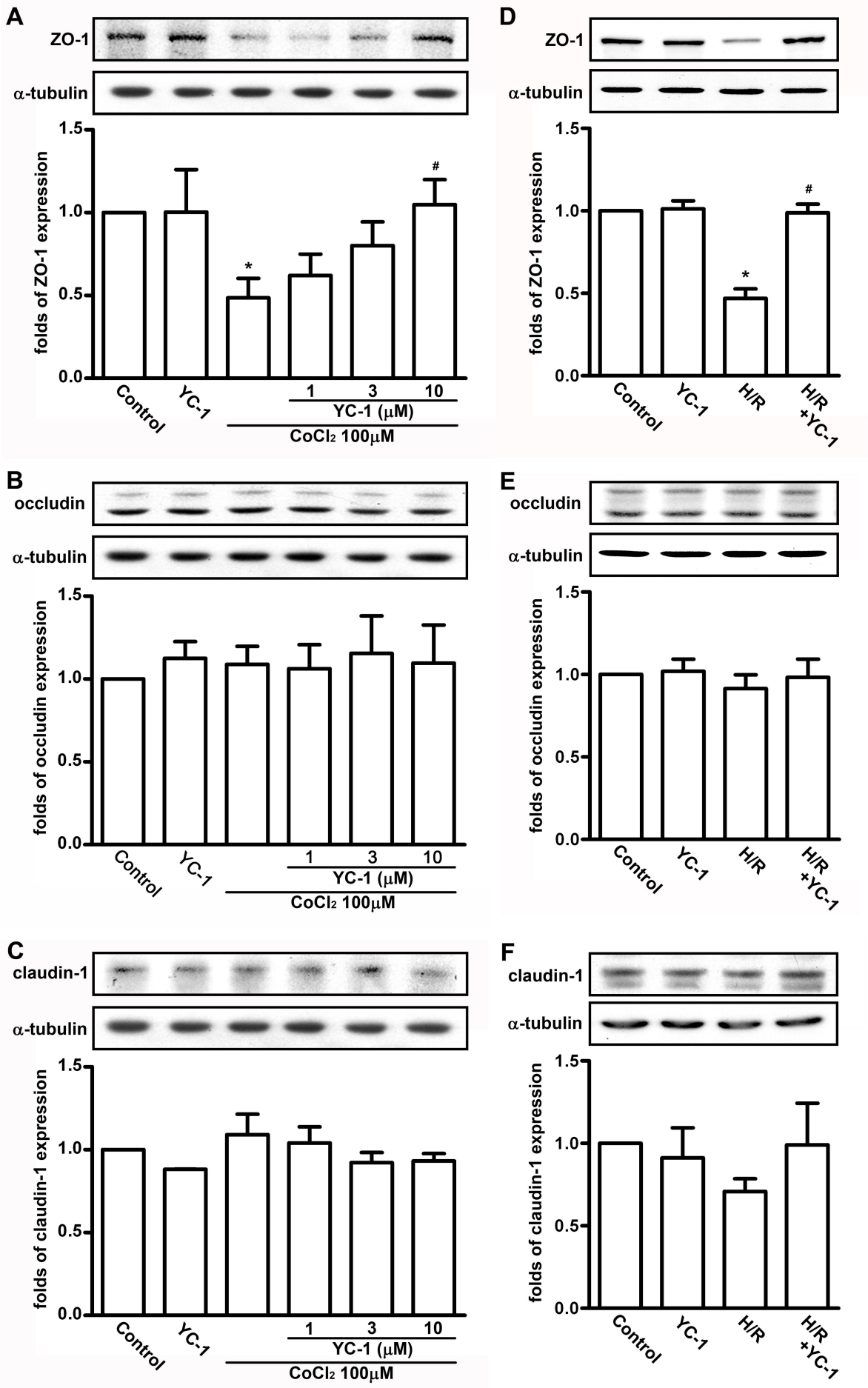
A
ZO-1
α-tubulin
folds of ZO-1 expression
1.5
1.0
0.5
0.0
*
#
Control
YC-1
1
3
10
YC-1 (μM)
CoCl2 100μM
D
ZO-1
α-tubulin
folds of ZO-1 expression
*
#
Control
YC-1
H/R
H/R +YC-1
B
occludin
α-tubulin
folds of occludin expression
Control
YC-1
1
3
10
YC-1 (μM)
CoCl2 100μM
E
occludin
α-tubulin
folds of occludin expression
Control
YC-1
H/R
H/R +YC-1
C
claudin-1
α-tubulin
folds of claudin-1 expression
Control
YC-1
1
3
10
YC-1 (μM)
CoCl2 100μM
F
claudin-1
α-tubulin
folds of claudin-1 expression
Control
YC-1
H/R
H/R +YC-1

Figure 3.

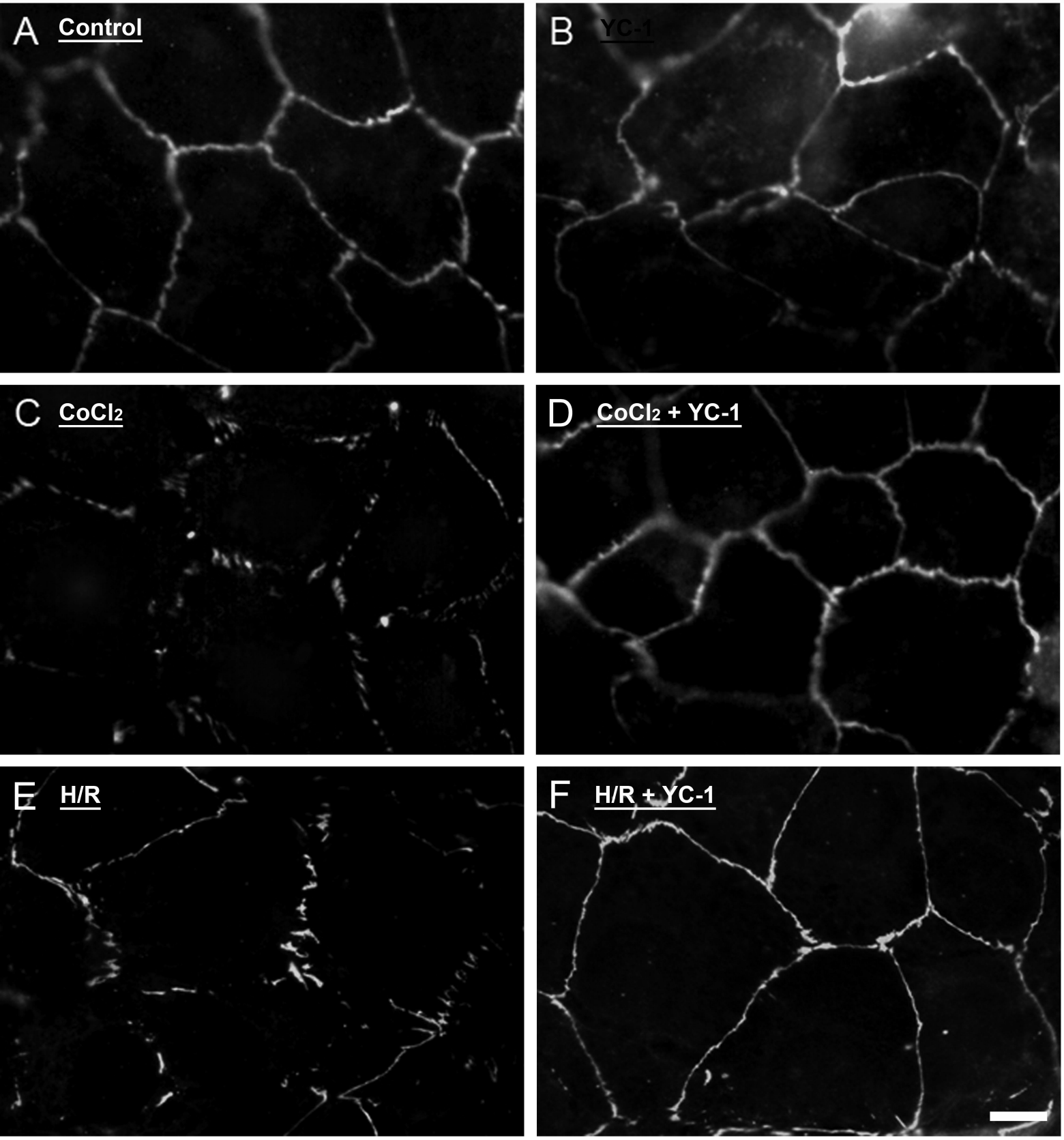

Figure 4.

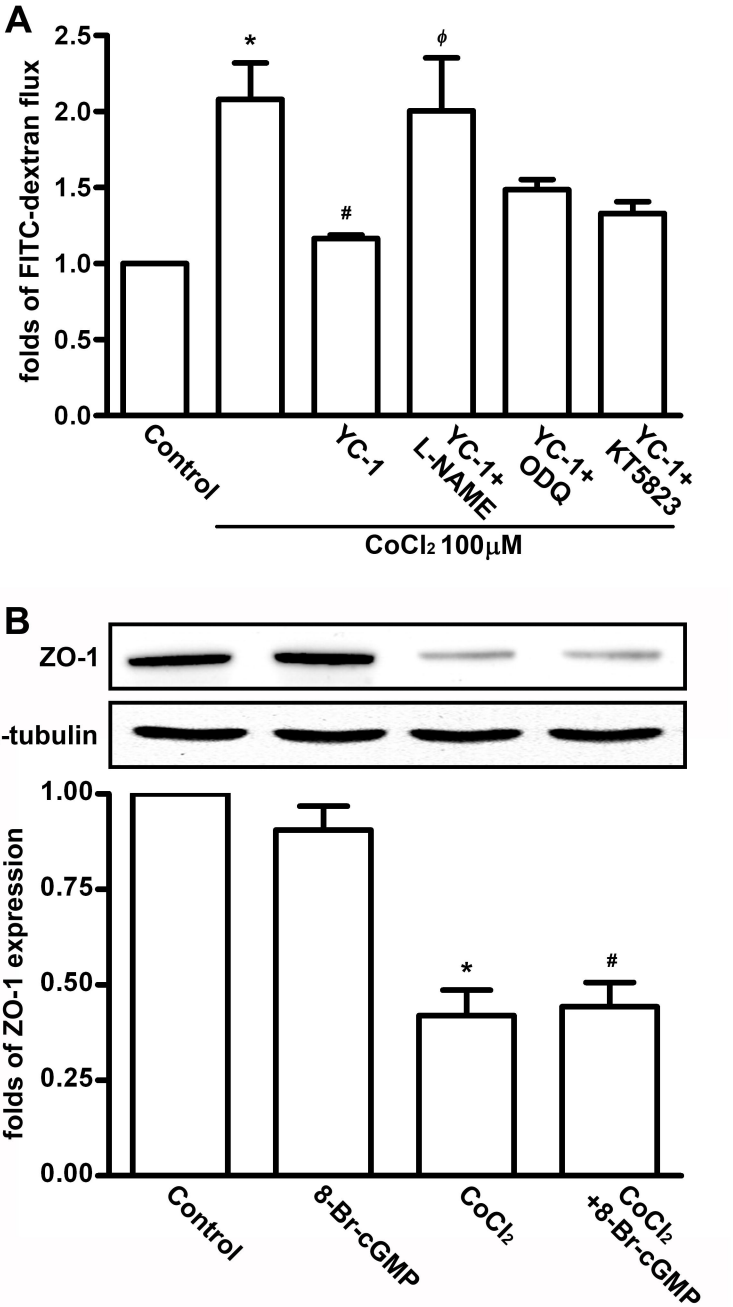
A
folds of FITC-dextran flux
2.5
2.0
1.5
1.0
0.5
0.0
*
#
ϕ
Control
YC-1
YC-1+ L-NAME
YC-1+ ODQ
YC-1+ KT5823
CoCl2 100μM
B
ZO-1
α-tubulin
folds of ZO-1 expression
1.00
0.75
0.50
0.25
0.00
*
#
Control
8-Br-cGMP
CoCl2
CoCl2 +8-Br-cGMP

Figure 5.

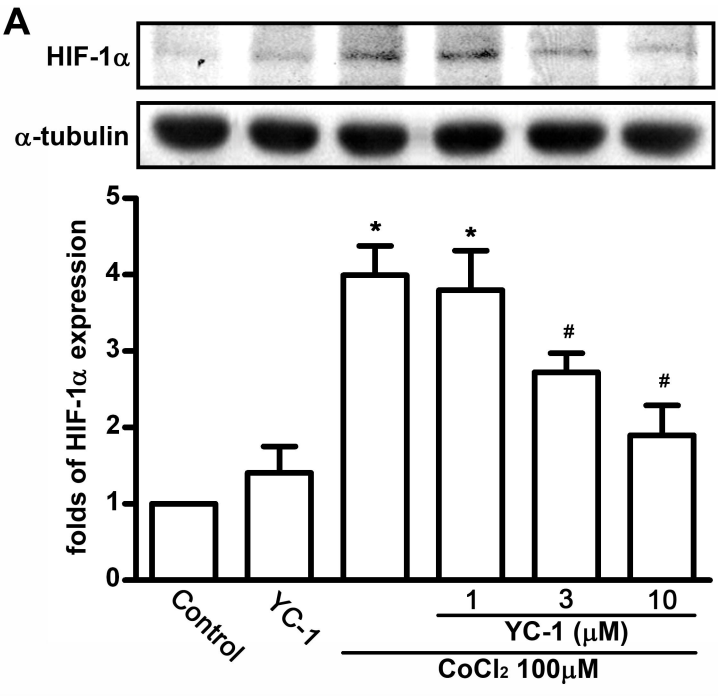
A
HIF-1α
α-tubulin
folds of HIF-1α expression
0
1
2
3
4
5
*
*
#
#
Control
YC-1
1
3
10
YC-1 (μM)
CoCl2 100μM

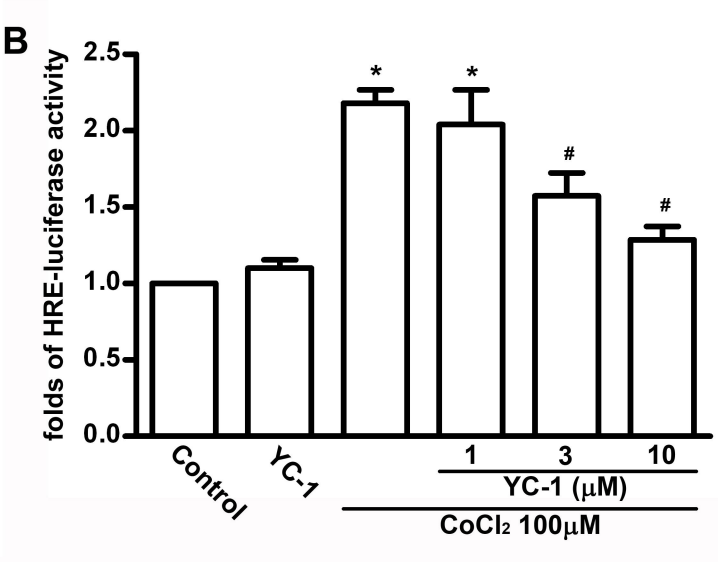
B
folds of HRE-luciferase activity
0.0
0.5
1.0
1.5
2.0
2.5
*
*
#
#
Control
YC-1
1
3
10
YC-1 (μM)
CoCl2 100μM

Figure 6.

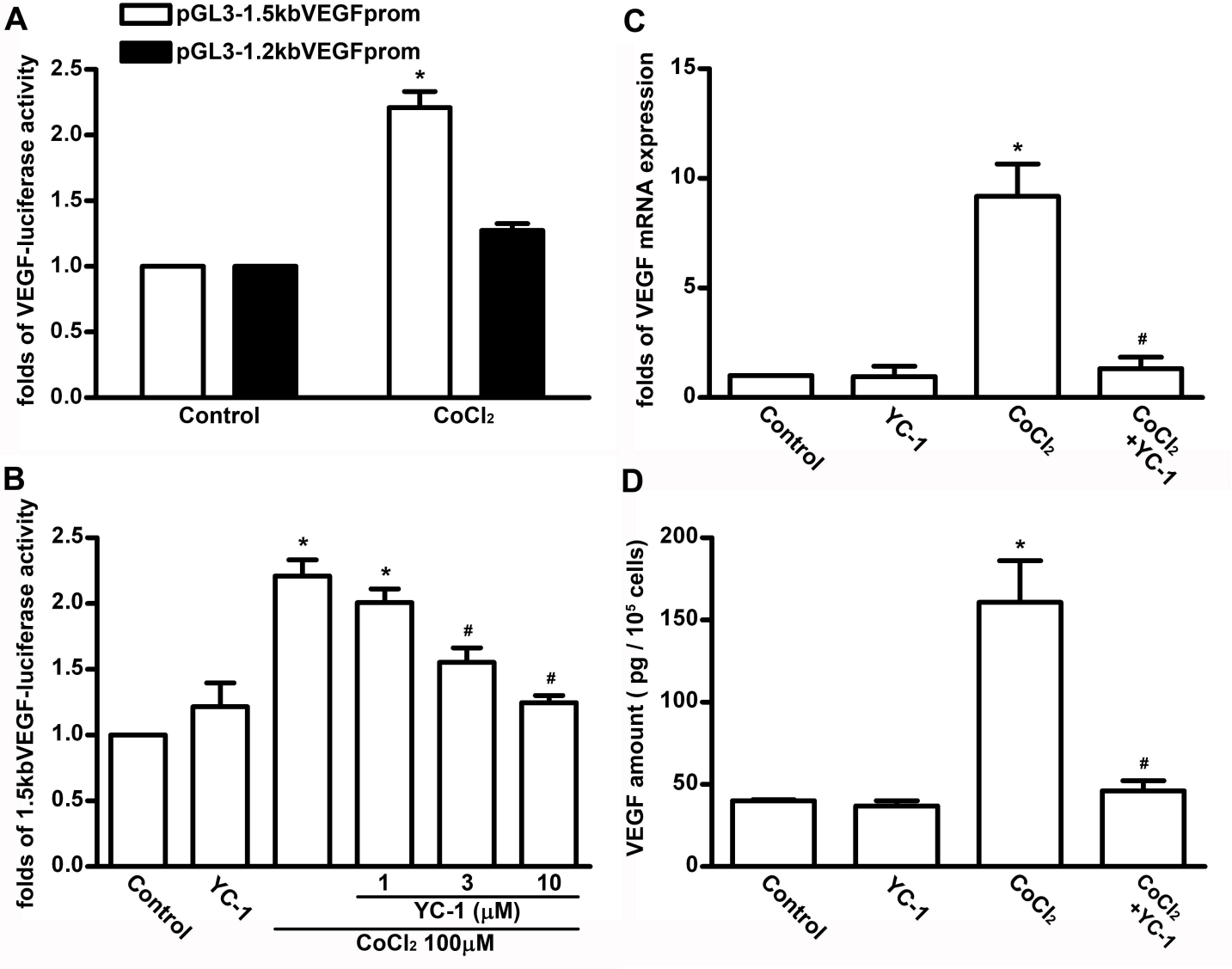
A
pGL3-1.5kbVEGFprom
pGL3-1.2kbVEGFprom
folds of VEGF-luciferase activity
2.5
2.0
1.5
1.0
0.5
0.0
*
Control
CoCl2
C
folds of VEGF mRNA expression
15
10
5
0
*
#
Control
YC-1
CoCl2
CoCl2 +YC-1
B
folds of 1.5kbVEGF-luciferase activity
2.5
2.0
1.5
1.0
0.5
0.0
*
*
#
#
Control
YC-1
1
3
10
YC-1 (μM)
CoCl2 100μM
D
VEGF amount (pg / 10^5 cells)
200
150
100
50
0
*
#
Control
YC-1
CoCl2
CoCl2 +YC-1

Figure 7.

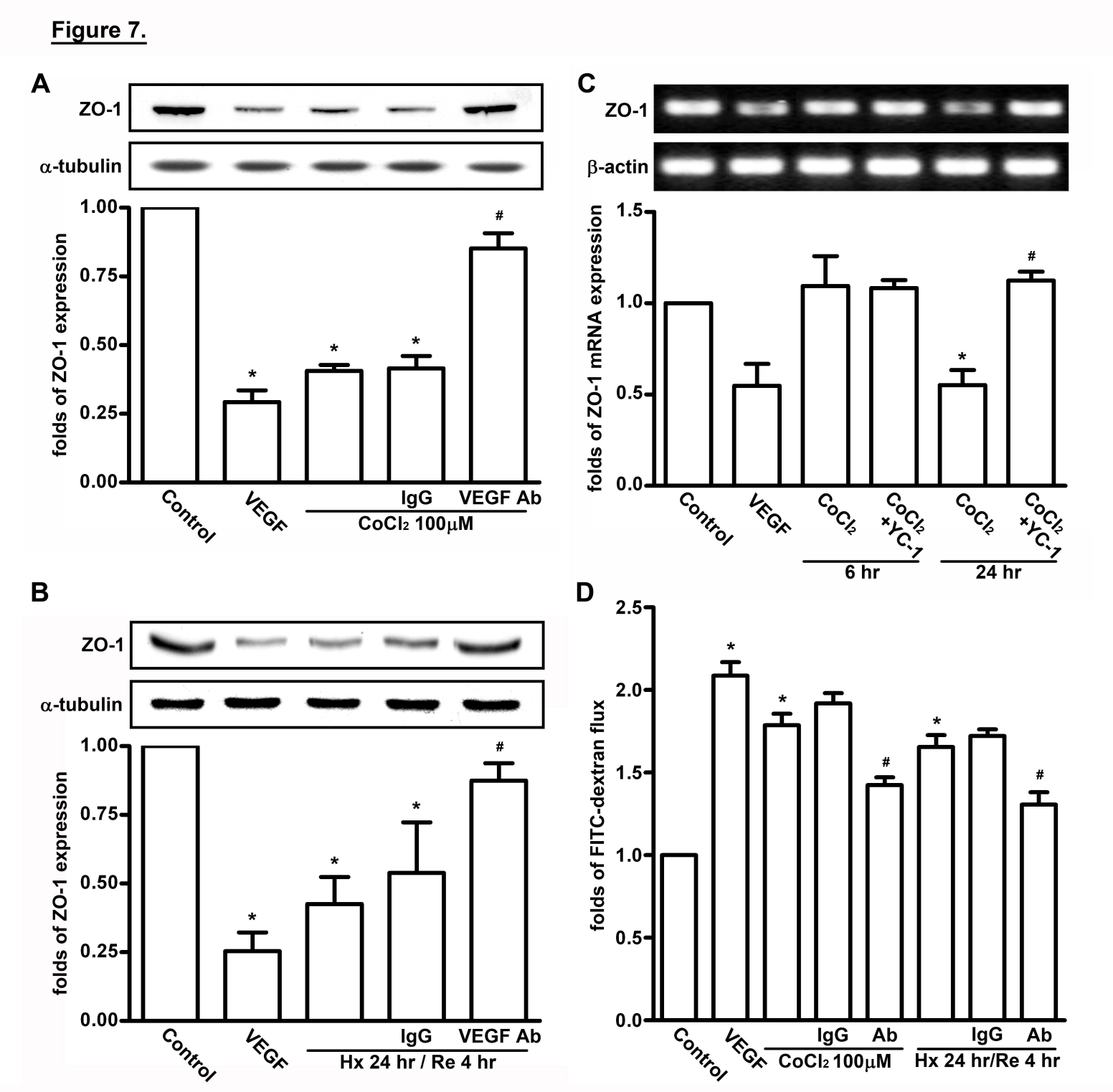
A
ZO-1
α-tubulin
folds of ZO-1 expression
1.00
0.75
0.50
0.25
0.00
Control
VEGF
IgG
VEGF Ab
CoCl2 100μM
B
ZO-1
α-tubulin
folds of ZO-1 expression
Control
VEGF
IgG
VEGF Ab
Hx 24 hr / Re 4 hr
C
ZO-1
β-actin
folds of ZO-1 mRNA expression
1.5
1.0
0.5
0.0
Control
VEGF
CoCl2
CoCl2 +YC-1
CoCl2
CoCl2 +YC-1
6 hr
24 hr
D
folds of FITC-dextran flux
2.5
2.0
1.5
1.0
0.5
0.0
Control
VEGF
IgG
Ab
CoCl2 100μM
IgG
Ab
Hx 24 hr/Re 4 hr

Figure 8.

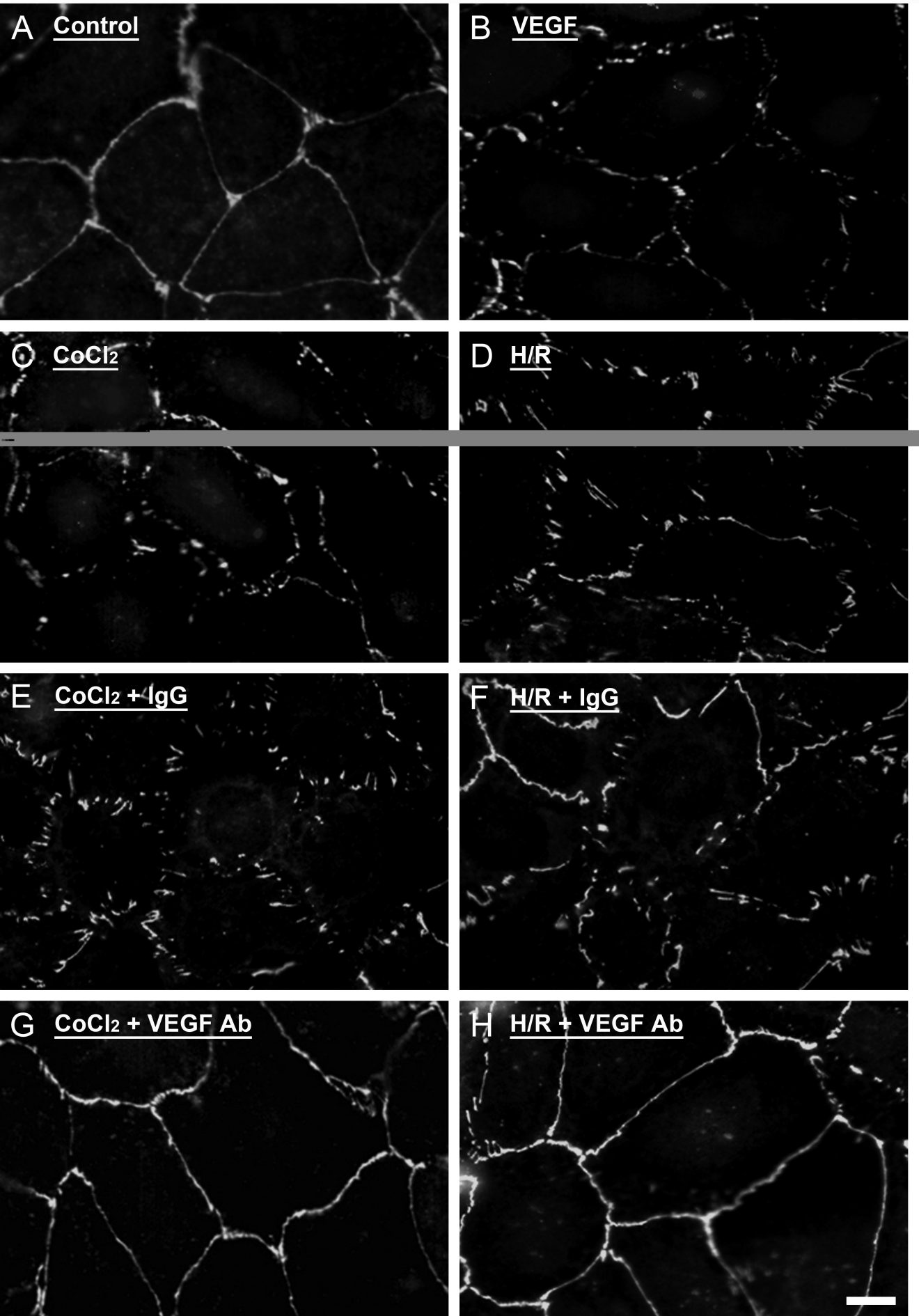
A Control
B VEGF
C CoCl2
D H/R
E CoCl2 + IgG
F H/R + IgG
G CoCl2 + VEGF Ab
H H/R + VEGF Ab

Figure 9.

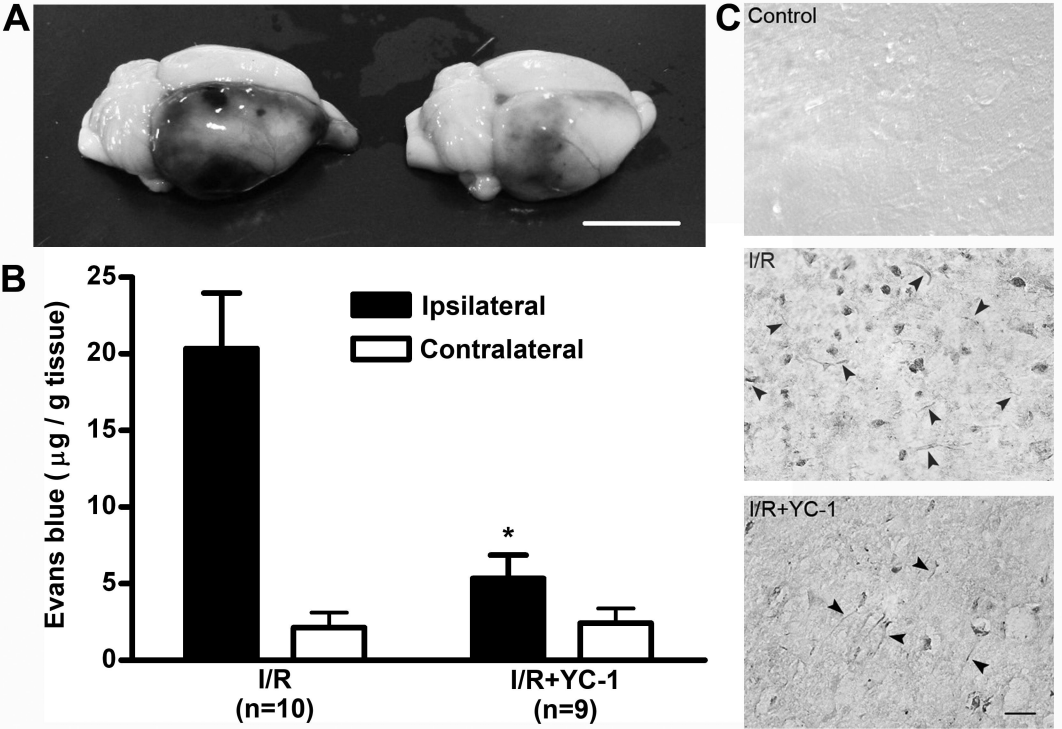
A
B
Evans blue (μg / g tissue)
25
20
15
10
5
0
Ipsilateral
Contralateral
*
I/R
(n=10)
I/R+YC-1
(n=9)
C
Control
I/R
I/R+YC-1